PROCEEDINGS, 41st Workshop on Geothermal Reservoir Engineering
Stanford University, Stanford, California, February 22-24, 2016
SGP-TR-209

A Reduced Form Representation of Temperature Drawdown in Sedimentary Basin Geothermal Reservoirs for the Development of Optimal Management Strategies

Iti H. Patel[1], Jeffrey M. Bielicki[1*], Thomas A. Buscheck[2]

1The Ohio State University, 2070 Neil Avenue, Columbus, OH 43210

2 Lawrence Livermore National Lab, Livermore, CA 94550, USA

*bielicki.2@osu.edu

Keywords: reservoir simulations, temperature drawdown, natural resource economics

ABSTRACT

A geothermal resource is often considered to be sustainable if the temperature within the reservoir is maintained at a level that can provide cost-effective heat. But, the heat that is extracted from the geothermal resource is used to provide a service to society and an economic gain to the provider of that service. In this context, sustainability entails simultaneously considering the rate at which the reservoir temperature renews and the rate at which heat is extracted and converted into economic profit. We developed a reduced form representation of temperature drawdown in sedimentary basin geothermal reservoirs for future development of optimal heat extraction strategies that incorporate physical and economic tradeoffs. We used the Non-isothermal Unsaturated-saturated Flow and Transport (NUFT) model to simulate the performance of a sedimentary geothermal reservoir under a variety of geologic conditions and operational scenarios and developed a reduced form representation of the drawdown and regeneration of reservoir. This representation can be integrated into a natural resource economics model to determine the mass flowrate that maximizes the net present profit given the performance of the geothermal resource.

INTRODUCTION

One limitation of geothermal energy is that the temperature of the resource can be depleted over time if the rate of heat extraction exceeds the rate at which natural geothermal heat flux increases the temperature in the reservoir. A common environmental viewpoint on sustainability entails maintaining a constant temperature of the produced fluid by extracting energy at a rate that is at or below the natural recharge rate of energy into the reservoir (Axelsson and Stefansson, 2003). But to the business owner of a geothermal system, a sustainable management strategy will provide the highest economic return on investment, which may result in speedy extraction of energy. The former perspective may be practical for low-temperature geothermal heat pumps, but it is not economically viable for geothermal energy for electricity production that may drawdown the temperature of the reservoir (Sanyal, 2005). Geothermal heat is renewable, where practical renewal of temperature (90-97%) after continuous production from a reservoir takes approximately five times the period of extraction time (Rybach et al., 2000). Resource depletion, then, is a question of how to manage the resource extraction more than a question of resource renewability (Bromley et al., 2006). While both environmental and economic perspectives highlight issues that are central to geothermal heat extraction, a more encompassing view on sustainability considers both the resource depletion and economic profit.

Natural resource economics is an integrated approach to resource management because it incorporates the interaction between environmental processes and the market. Optimal control approaches have been extensively studied for management of fisheries and forests (Bonfil, 2005; Tahvonen et al., 2010; Weitzman, 2003) in order to determine the optimal time-path of extraction of a renewable resource. This comparison of geothermal energy to a fishery has been made previously to elucidate the ideas of renewability and sustainability, but the natural resource economic approach has not been applied to the extraction of geothermal heat (Stefansson, 2000). A considerable portion of such a resource management model involves determining the temperature of the produced fluid as energy is being extracted from the reservoir. The change in temperature depends in part on a variety of variables, including reservoir parameters that affect the rate at which heat transfer takes place within the reservoir. As such, this paper investigates the renewability of reservoir temperature, specifically for sedimentary basin geothermal resources which are emerging candidates for geothermal development in part because to their enormous fluid capacity and high temperatures (Cacace et al., 2010; Fridleifsson et al., 2008). Particularly, this paper develops a reduced form representation of the change in the temperature of the produced fluid as a component of a natural resource economic model for a geothermal resource.

METHODS

Model of Sedimentary Basin Geothermal Reservoir Performance

We used the Non-isothermal Unsaturated-saturated Flow and Transport (NUFT) code to simulate the physical performance of sedimentary basin geothermal reservoirs (Hao et al., 2011). NUFT integrates the finite difference method, spatial discretization, and the Newton-Raphson method to solve the conservation of mass and energy equations at each time step. The code contains distinct modules and we used the multi-phase multi-component flow with a thermal option (Nitao and Sun, 2015) in order to have fluid parameters that vary with temperature.

We implemented a radially symmetric R-z model with a vertical column of elements that represent a perforated central injection well and an element that represents a perforated radial production well. The porous and permeable reservoir was modeled as a laterally unconfined aquifer that is confined by an impervious caprock above the reservoir and an impervious bedrock below the reservoir with that properties are similar to typical sandstones and have been used in previous papers that investigated CO_2 injection into deep saline aquifers for sequestration from the atmosphere and for geothermal energy production using CO_2 and native brine (Birkholzer et al., 2009; Buscheck et al., 2013). Similar R-z configurations have been used in previous modeling studies that simulate the performance of sedimentary basin geothermal reservoirs (Adams et al., 2015, 2014; Garapati et al., 2015, 2014; Saar et al., 2015). Each simulation is for an unconfined reservoir with a vertical injection well and radial production well, where the injection well and the production well is separated by a radial distance of 700 m.

We conducted numerous reservoir simulations with NUFT; each simulation used a distinct combination of reservoir top depth, reservoir thickness, reservoir permeability, and geothermal temperature gradient. The parameters we chose for the simulations cover a range of the characteristics of sedimentary basins in the United States and have been investigated in previous studies of sedimentary basin geothermal energy production and CO_2 storage (Anderson, 2013). We used water as the heat extraction fluid in the reservoir simulations we conducted, and set the mass flowrate of the injection well equal to the mass flowrate of the production well. The physical parameters for the reservoir, the confining unit, and the heat extraction fluid for the models that were simulated in NUFT are included in Table 1. The fluid properties of the water that is injected into the reservoir are determined from the ASME steam tables built into the NUFT code, using the pressure and temperate of the element in the mesh (ASME, 2006).

Table 1: Reservoir Parameters for Sedimentary Basin Geothermal Reservoir Simulations Using the NUFT Code

Parameter	Parameter Value
Permeability [m^2]:	
Reservoir, κ_r	10^{-11}, 10^{-12}, 10^{-13}, $5x10^{-14}$, 10^{-14}, $5x10^{-15}$
Confining Unit, κ_c	10^{-18}
Porosity:	
Reservoir, ϕ_r	0.10
Confining Unit, ϕ_c	0.10
Density [kg/m^3]:	
Reservoir, ρ_r	920
Confining Unit, ρ_c	920
Compressibility [Pa^{-1}]:	
Reservoir, β_r	$4.5x10^{-10}$
Confining Unit, β_c	$4.5x10^{-10}$
Specific Heat: [kJ/kg-K]	
Reservoir, $c_{p,r}$	2.8
Confining Unit, $c_{p,r}$	2.8
Thermal Conductivity [W/m-K]:	
Reservoir, k_r	2.0
Confining Unit, k_c	2.0
Reservoir Dimensions [m]	
Top Depth, z	2500, 3500, 5000
Thickness, Δz	50,100
Temperature Gradient, G [°C/km]	35, 50
Mass Flowrate, $\dot{m}_f$ [kg/s]	5, 10, 25, 50, 100, 150, 200, 250

Reservoir Performance and Normalization

To conduct a reservoir simulation, we set the surface temperature (at z = 0 m) to 15 ^oC and calibrated the model so that the elements in the mesh were in thermal and hydrostatic equilibrium. We then simulated constant fluid injection and fluid production for 200 years. The NUFT model determined the temperature (T_{inj}) of this injected fluid that corresponds to the specified enthalpy that was specified for the pressure at the injection well. We recorded temperature, pressure, and heat flow into the reservoir for each element in the mesh at each time step.

The enthalpy that is extracted from the reservoir through the production well during a period of time, Δt, at a time t, is:

$$Q_t = \dot{m} \cdot c_{p,t} \cdot (T_{prod,t} - T_{inj,t}) \cdot \Delta t \quad (1)$$

where $\dot{m}_t$ is the mass flowrate of the fluid per unit of time [kg/s], Δt that is produced from the reservoir at time t [s], $c_{p,t}$ is the specific heat of the produced fluid [kJ/kg-K], $T_{prod,t}$ is the temperature of the produced fluid at time t [K], and $T_{inj,t}$ is the temperature of the injected fluid at time t [K]. For a given combination of reservoir parameters, the temperature of the fluid being produced from the reservoir ($T_{prod,t}$) will change over time as a function of how much heat has been extracted from the reservoir through the production well and how much heat has been added to the reservoir from the natural geothermal heat flux. The geothermal temperature gradient is a function of the natural heat flux (q) and the thermal conductivity of the rock (k_{rock}): $q = k_{rock} G$. In order to produce a model that is generalizable across various geologic settings and operational decisions, we combined the results of the 300 reservoir simulations by fitting a generalized logistic curve to dimensionless normalizations of the temperature of the produced fluid ($\bar{T}$) and of the energy that is extracted from the reservoir ($\bar{Q}$). This logistic curve of the form in equation 2, also known as Richards' curve (Richards, 1959), thus serves as a reduced form representation of the performance of a sedimentary basin geothermal reservoir for a range of reservoir parameters and operational decisions:

$$\overline{T} = U + \frac{L - U}{(1 + Ae^{-x(\overline{Q} - M)})^{1/v}} \quad (2)$$

The dimensionless normalized production temperature ($\overline{T}$) in equation 3 is the difference between the temperature of the produced fluid and of the injected fluid divided by the difference between the initial temperature of the produced fluid and the temperature of the injected fluid.

$$\overline{T} = \frac{T_{prod,t} - T_{inj}}{T_{prod,t=0} - T_{inj}} \quad (3)$$

The initial temperature of the produced fluid is a function of the depth of the top of the reservoir (z), the geothermal temperature gradient (G), and surface temperature (T_s): $T_{prod,t=0} = T_s + zG$. Since the temperature of the produced fluid at any point in time can never exceed its initial temperature or be below the injection temperature, $0 \leq \overline{T} \leq 1$. The upper asymptote of the logistic curve in equation 4, U, was set to one, because the normalization of temperature ($\bar{T}$) cannot be greater than one.

To construct a dimensionless normalization of the energy that is extracted from the reservoir at time t ($\overline{Q}_t$), we calculated the cumulative amount of energy that has been extracted from the reservoir, using Q_t in equation 1 for each time increment, and divided that value by the total amount of energy that could have been extracted from the reservoir ($Q_{tot,t}$). Since the cumulative amount of energy that is extracted from the reservoir cannot be greater than the total amount of energy that could be extracted from the reservoir, $0 \leq \bar{Q}_t \leq 1$.

$$\overline{Q}_t = \frac{\sum_{t=0}^{t} Q_t}{Q_{tot,t}} = \frac{\sum_{t=0}^{t} Q_t}{Q_{res,t=0} + \sum_{t=0}^{t} Q_{in,t} + \sum_{t=0}^{t} Q_t} \quad (4)$$

where $Q_{res,t=0}$ is the initial amount of energy that is in the reservoir at t=0 [kJ], and $Q_{in,t}$ is the net amount of energy that enters the reservoir due to the natural geothermal heat flux during each time step at time t. The initial amount of energy that is in the reservoir at t=0 is,

$$Q_{res,t=0} = \pi r^2 \cdot \Delta z \cdot T_{ave,r,t=0} \cdot [(1 - \theta_r) \cdot \rho_r \cdot c_{p,r} + \theta_r \cdot \rho_f \cdot c_{p,f}] \quad (5)$$

where r is the radius of the geothermal reservoir [m], ρ_r and ρ_f are the densities of the reservoir rock and the fluid in the pores of the reservoir, respectively [kg/m^3], $c_{p,r}$ and $c_{p,f}$ are the heat capacities of the reservoir rock and the fluid in the pores of the reservoir, respectively [kJ/kg-K], and $T_{ave,r,t=0}$ is the average temperature in the reservoir at t=0: $T_{ave,r,t=0} = T_s + G \cdot (z + \frac{\Delta z}{2})$.

Since the NUFT model is in thermal equilibrium at the beginning of the simulation, there will be no net heat transfer into the reservoir from the geothermal heat flux at t=0. The geothermal heat flux will begin to add heat to the reservoir when the temperature in the reservoir decreases due to the injection of fluid that is colder than the reservoir ($T_{inj} < T_r$) and fluid that has been heated in the reservoir is produced from the reservoir.

Since the temperature of the reservoir varies within the reservoir, we summed the net heat flow into the reservoir that was recorded for each element around the perimeter of the reservoir to determine $Q_{in,t}$. This net amount of heat that is added to the reservoir will depend on a variety of reservoir characteristics and operational decisions (e.g., the history of heat extraction and the resulting distributions of temperature and pressure in the reservoir, the physical attributes of the reservoir, the type and size of the production system; expanded

from Rybach (2007)). We thus performed a maximum likelihood panel regression on the data generated by NUFT across all of the simulations in order to produce a reduced form representation of $Q_{in,t}$. The regression was of the form,

$$\sum_{t=0}^{t} Q_{in,t} = \kappa^{\beta_1} \cdot z^{\beta_2} \cdot \Delta z^{\beta_3} \cdot \dot{m}^{\beta_4} \cdot G^{\beta_5} \cdot \left(\sum_{t=0}^{t} Q_t\right)^{\beta_6} \tag{6}$$

where β_1, β_2, β_3, β_4, β_5, and β_6 are the parameters that were estimated by the regression.

GEOTHERMAL RESERVOIR PERFORMANCE

We used the data that was generated in every NUFT simulation to determine $\bar{T}$ and $\bar{Q}$. Figure 1 shows these data for all the depths combined and separated by the depth of the reservoir that was used in the simulation. The normalized data for each depth trace out the same general trend. We then estimated the parameters that fit the logistic curve in equation 2 to the normalized data, which is shown in red that fit the logistic curve to all of the normalized data.

$$T_{prod,s} = \left[1 - \frac{0.8682}{\left(1 + 42.46\, e^{-49.50\,(\bar{Q}_s - 0.8986)}\right)^{1/4.1}}\right]\left(T_{prod,\tau=0} - T_{inj}\right) + T_{inj} \tag{7}$$

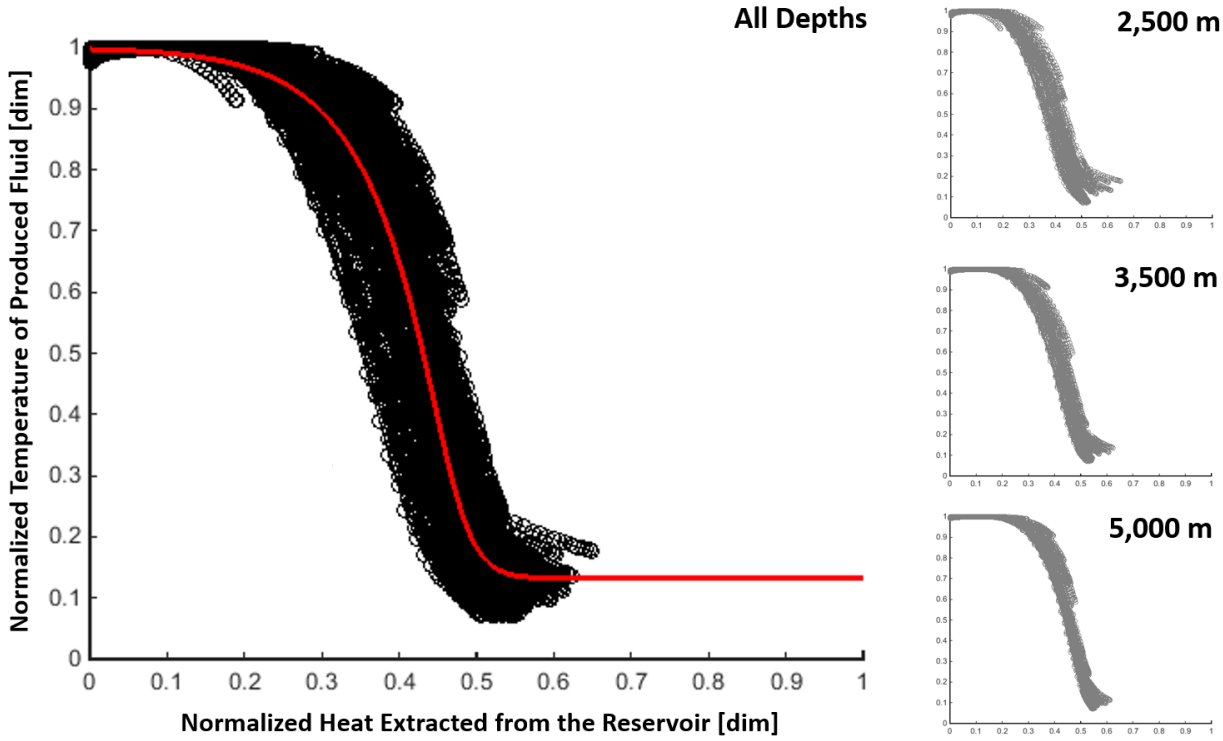

Figure 1: Normalization of the Temperature of Produced Fluid as a Function of the Energy that has been Extracted from the Reservoir

We also used the data generated by NUFT to estimate the parameters in equation 6 that relate $Q_{in,t}$ to Q_t. The net amount of heat that enters the reservoir at a point in time, $Q_{in,t}$, depends on the difference in temperature between each element on the inside boundary of the reservoir and the neighboring element(s) on the outside boundary of the reservoir. When heat is extracted from the reservoir, the temperature of the elements inside the reservoir will be decrease below the state at which they are in thermal equilibrium with the surrounding rock. As such, reservoir temperature recharge from the geothermal heat flux will occur only when heat has been extracted from the reservoir. Table 2 shows estimated coefficients from the regression. We transformed equation 6 into a linear model by taking the natural logarithm of both sides. The parameter for mass flowrate (β_4 in equation 6) was not significant (Table 2) because it is already contained in Q_t (equation 1).

Table 2: Maximum Likelihood Estimates of Panel Regression of Equation 6. Standard errors are in parentheses.

Coefficient	Estimated Value
β1	0.154*** (0.0071)
β2	-0.200*** (0.0419)
β3	1.061** (0.0452)
β4	0.003 (0.0139)
β5	-0.362*** (0.0716)
β6	-0.766*** (0.0014)
*** p<0.01; ** p< 0.05; *p<0.10	

Figure 2 shows the percent of Q_{in} and marginal energy extracted over time relative to the total marginal amount of energy that could be extracted from the reservoir, Q_{tot}, for four case studies with different temperature gradients, depths, and mass flowrates. All four scenarios follow the same general pattern, where the energy that is extracted and net energy into the reservoir are initially zero. As constant injection and production of fluid takes place, the amount of energy that is extracted comprises the majority of the incremental amount energy that could be extracted in a time period. Over time, the net energy into the reservoir increases as heat transfer through conduction and convection takes place. The percent of net energy into the reservoir and energy extracted asymptote over time. The difference between the scenarios in Figure 2 is where this asymptote is. The distance between the asymptote of the two components is larger with increasing mass flowrate, depth, and temperature gradient as seen when comparing Figure 2(a) and Figure 2(c) for mass flowrate and Figure 2(a) and Figure 2(b) for depth and temperature gradient. At lower mass flowrates, the geothermal heat flux reheats the reservoir more effectively than when more energy is extracted. But this heat transfer into the reservoir is limited by the thermal conductivity of the rocks and temperature difference between the surrounding rock and the rock within the reservoir. As such, a larger mass flowrate increases the amount of energy that is extracted from the reservoir but not at the same magnitude as the net amount of energy that enters the reservoir. Similarly, the temperature of the reservoir increases with increasing depth and temperature gradient, which allows more energy to be extracted for a given mass flowrate. These effects are most apparent when comparing Figure 2(a) and Figure 2(d).

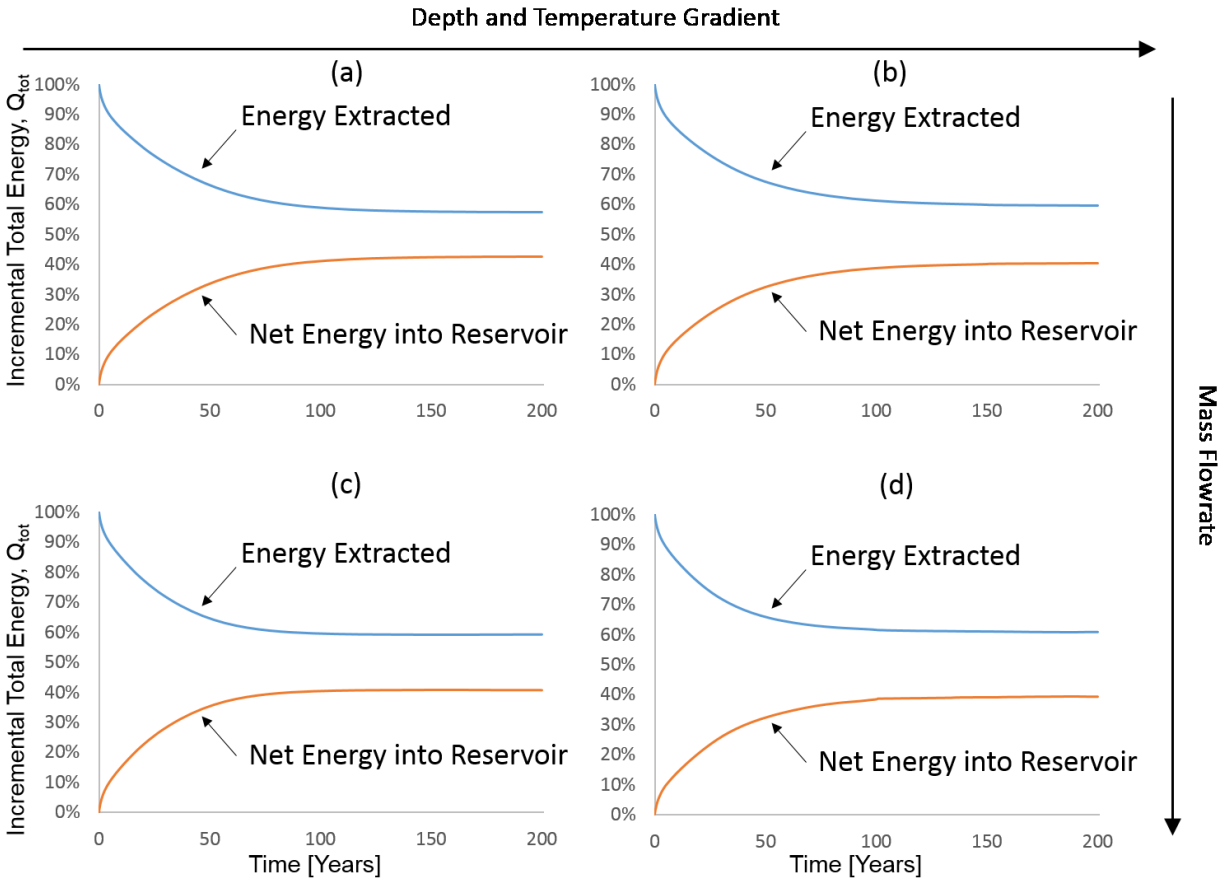

Figure 2: Components of Energy Extracted Normalization for Four Cases. (a) Depth, z = 2500m, Temperature Gradient, G = 35°C/km, Mass Flowrate, $\dot{m}$ = 100 kg/s. (b) Depth, z = 5000m, Temperature Gradient, G = 50°C/km, Mass Flowrate, $\dot{m}$ = 100 kg/s. (c) Depth, z = 2500m, Temperature Gradient, G = 35°C/km, Mass Flowrate, $\dot{m}$ = 150 kg/s. (d) Depth, z = 5000m, Temperature Gradient, G = 50°C/km, Mass Flowrate, $\dot{m}$ = 150 kg/s. All Cases: Permeability, $\kappa = 10^{-12}$ m^2, Thickness, Δz = 100m.

The energy "recharge" rate of the reservoir, Ψ_s, is the net energy that enters the reservoir during a single time period (t) as a function of the total energy that could be extracted from the reservoir. For example, when the recharge rate is 100%, the geothermal heat flux adds the same amount of energy to the reservoir as is extracted from the reservoir. As such the temperature of the produced fluid is not affected. In contrast, there is no energy entering the reservoir when the recharge rate is 0%:

$$\Psi_t = \frac{Q_{in,t}}{Q_{tot,t}} = \frac{Q_{in,t}}{Q_{res,t=0} + \sum_{t=1}^{t} Q_{in,t} + Q_t} \tag{8}$$

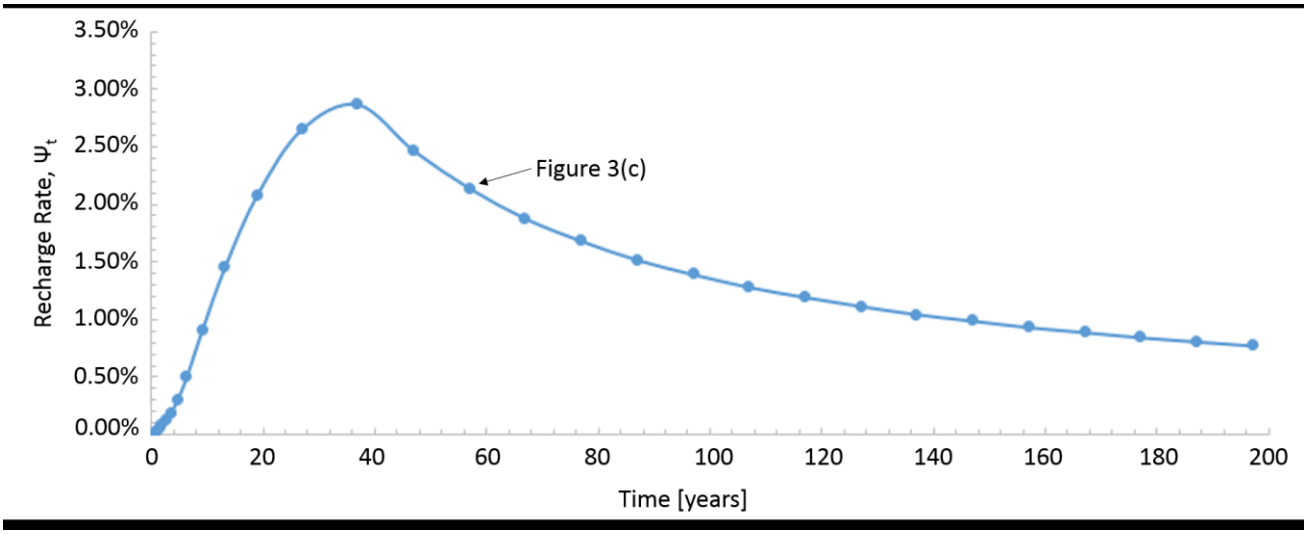

Figure 3: Recharge rate of Scenarios Given in Figure 2. (See Figure 3 caption)

Figure 3 shows the recharge rate over time for the scenario in Figure 2(c). This scenario has the highest recharge rate of all of the scenarios shown in Figure 2, with a maximum of 2.87%. This recharge rate is likely to be small when compared to interest rates that would be used in time value of money calculations for capital investment decisions.

CONCLUSION

After the recharge rate has peaked, the recharge rate steadily decreases over time because the rock surrounding the reservoir has cooled. This implies that the temperature in the reservoir will take longer to recharge because a larger volume of the rock has lost heat. This cooling of the surrounding reservoir rock is an important factor for determining optimal management strategies of sedimentary basin geothermal resources. Since the maximum recharge rate is low and likely to be less than interest rates, a natural resource economics approach suggests that it may be optimal to extract heat from the reservoir to draw down the reservoir temperature as quickly as possible, and let the profit that has been generated by this heat compound at a higher rate than the reservoir would regenerate.

ACKNOWLEDGEMENTS

This research is funded by a grant from the U.S. National Science Foundation Sustainable Energy Pathways program (1230691). I.H.P. developed the methodology, conducted analyses, analyzed results, and wrote the paper. J.M.B. developed the methodology, analyzed results, and wrote the paper.

REFERENCES

Adams, B.M., Kuehn, T.H., Bielicki, J.M., Randolph, J.B., Saar, M.O., 2015. A Comparison of Electric Power Output of CO_2 Plume Geothermal (CPG) and Brine Geothermal Systems for Varying Reservoir Conditions. Appl. Energy 140, 365–377. doi:10.1016/j.apenergy.2014.11.043

Adams, B.M., Kuehn, T.H., Bielicki, J.M., Randolph, J.B., Saar, M.O., 2014. On the importance of the thermosiphon effect in CPG (CO_2 plume geothermal) power systems. Energy 69, 409–418. doi:10.1016/j.energy.2014.03.032

Anderson, T.C., 2013. Geothermal Potential of Deep Sedimentary Basins in the United States 37.

ASME, 2006. ASME Steam Tables Compact Edition. Three Park Avenue, New York, NY, USA.

Axelsson, G., Stefansson, V., 2003. Sustainable Management of Geothermal Resources. Int. Geotherm. Conf. Reykjavík 40–48.

Birkholzer, J., Zhou, Q., Tsang, C., 2009. Large-scale impact of CO_2 storage in deep saline aquifers: A sensitivity study on pressure response in stratified systems. Int. J. Greenh. Gas Control 3, 181–194. doi:10.1016/j.ijggc.2008.08.002

Bonfil, R., 2005. Fishery Stock Assessment Models and their Application to Sharks, in: Management Techniques for Elasmobranch Fisheries. pp. 154–181.

Bromley, C.J., Mongillo, M., Rybach, L., 2006. Sustainable utilization strategies and promotion of beneficial environmental effects–Having your cake and eating it too. Proc. World Geotherm. Congr.

Buscheck, T.A., Chen, M., Lu, C., Sun, Y., Hao, Y., Elliot, T.R., Choi, H., Bielicki, J.M., 2013. Analysis of Operation Strategies for Utilizing CO2 for Geothermal Energy Production, in: Workshop on Geothermal Reservoir Engineering Stanford University. Stanford, California.

Cacace, M., Kaiser, B.O., Lewerenz, B., Scheck-Wenderoth, M., 2010. Geothermal energy in sedimentary basins: What we can learn

from regional numerical models. Chemie der Erde - Geochemistry 70, 33–46. doi:10.1016/j.chemer.2010.05.017

Fridleifsson, I.B., Bertani, R., Lund, J.W., Rybach, L., 2008. The possible role and contribution of geothermal energy to the mitigation of climate change, in: IPCC Scoping Meeting on Renewable Energy Source. pp. 59–80.

Garapati, N., Randolph, J.B., Saar, M.O., 2015. Brine displacement by CO2, energy extraction rates, and lifespan of a CO2 -limited CO2 -Plume Geothermal (CPG) system with a horizontal production well. Geothermics 55, 182–194. doi:10.1016/j.geothermics.2015.02.005

Garapati, N., Randolph, J.B., Valencia, J.L., Saar, M.O., 2014. CO2-Plume Geothermal (CPG) Heat Extraction in Multi-layered Geologic Reservoirs. Energy Procedia 63, 7631–7643. doi:10.1016/j.egypro.2014.11.797

Hao, Y., Sun, Y., Nitao, J.J., 2011. Overview of NUFT: Versatile Numerical Model for Simulating Flow and Reactive Transport in Porous Media. Groundw. React. Transp. Model. 213–240. doi:10.2174/97816080530631120101

Nitao, J.J., Sun, Y., 2015. USNT Reference Manual of the NUFT Code for Yucca Mountain Project.

Richards, F.J., 1959. A Flexible Growth Constant for Empirical use. J. Exp. Bot. 10, 290–300.

Rybach, L., 2007. Geothermal Sustainability, in: European Geothermal Congress. Zurich, Switzerland, pp. 1–7.

Rybach, L., Megel, T., Eugster, W.J., 2000. At what time scale are geothermal resources renewable? Proc. World Geotherm. Congr. 2000 Kyushu-Tohoku, Japan 867–872.

Saar, M.O., Buscheck, T.A., Jenny, P., Garapati, N., Randolph, J.B., Karvounis, D.C., Chen, M., Sun, Y., Bielicki, J.M., 2015. Numerical Study of Multi-Fluid and Multi-Level Geothermal System Performance. Proceedings, World Geotherm. Congr. 2015.

Sanyal, S.K., 2005. Sustainability and Renewability of Geothermal Power Capacity. Geotherm. Energy 24–29.

Stefansson, V., 2000. The Renewability of Geothermal Energy. World Geotherm. Congr. 883–888.

Tahvonen, O., Pukkala, T., Laiho, O., Lähde, E., Niinimäki, S., 2010. Optimal management of uneven-aged Norway spruce stands. For. Ecol. Manage. 260, 106–115. doi:10.1016/j.foreco.2010.04.006

Weitzman, M., 2003. Income, Wealth, and the Maximum Principle. Cambridge: Harvard University Press.